Swarm Robotics surveillance control with Ant Cellular Automata Model in the Cerrado Biome for preserving biodiversity

Heitor Castro Brasiel ⬛ [**Federal Institute of Triângulo Mineiro** | *heitor.brasiel@estudante.iftm.edu.br*]
Danielli Araújo Lima ⬛ ✉ [**Federal Institute of Triângulo Mineiro** | *danielli@iftm.edu.br*]

✉ *Laboratory of Intelligent Computing and Robotics (LICRO), Federal Institute of Education, Science and Technology of Triângulo Mineiro (IFTM) Campus Patrocínio, Av. Líria Terezinha Lassi Capuano - Universitário, Patrocínio - MG, 38747-792, Brazil.*

Abstract The Cerrado biome in Brazil plays a vital role in preserving biodiversity, providing essential ecosystem services, and supporting agriculture, making it a crucial and valuable natural resource. Sete Cidades National Park stands out for its rock formations, 10,000-year-old cave paintings and its Cerrado vegetation. The Cerrado is known for being a pyrobiome, so its patrolling becomes essential. In this context, this paper introduces a novel approach to swarm robotics patrolling in the unique ecosystem of the Sete Cidades National Park, located within the Cerrado biome. The study presents three distinct cellular automata models designed for the task, aiming to enhance the efficiency and coverage of patrolling efforts. The key difference between our model presented in this research and the previous one is our focus on a map that encompasses diverse vegetation types, specifically designed to represent the Sete Cidades National Park, with a primary goal of monitoring forest fires. The results demonstrated that the best-performing model was the Forest Tabu Inverted Ant Cellular Automata, which achieved an average of 21.77 complete patrol cycles with 95% confidence. This outcome was obtained using three robots, a tabu queue of $|Q| = 80$, and a maximum pheromone per cell equals to $\rho = 10^3$. These parameters highlight the efficacy of this model in optimizing patrol cycles and the efficient use of resources for environmental surveillance in the Sete Cidades National Park, particularly in the context of fire prevention.

Keywords: Swarm Robotics, Cellular Automata, Inverted Ants Pheromone, Environmental Surveillance, Sete Cidades National Park, Cerrado Biome, Interactive Patrol, Geographic Information System.

1 Introduction

Preserving the environment is crucial because it safeguards the delicate balance of ecosystems, sustains biodiversity, ensures clean air and water for all living beings, and ultimately secures a habitable planet for future generations (Alencar *et al.*, 2019). The Cerrado in Brazil, often referred to as "Brazil's savanna", is a remarkable and diverse biome known for its unique landscapes and rich biodiversity, making it a vital part of the country's natural heritage (Ferreira *et al.*, 2022a). It also plays a crucial role in preserving biodiversity, storing carbon, and providing essential ecosystem services, underlining its pivotal importance for both Brazil and the world (Lima and Lima, 2014). During the dry seasons of winter and fall, the Cerrado faces an increased risk of firespread, posing significant challenges to its unique ecosystem and underscoring the need for proactive fire management strategies (Ferreira *et al.*, 2022b). Therefore, it is very important to pay attention to these areas during these periods.

The Sete Cidades National Park is a valuable Brazilian conservation entity dedicated to the comprehensive protection of nature. It encompasses areas in the northern regions of Piauí, spanning across the municipalities of Brasileira and Piracuruca (Alvarado *et al.*, 2019; Gaia *et al.*, 2022). This natural gem plays a pivotal role in conserving the area's wealth and biodiversity. The park's distinctive landscapes and ecosystems have been meticulously studied, revealing six distinct vegetation types/classes ($|C_k| = 6$): Riparian Forest, Evergreen Forest, Dense Cerrado, Typical Cerrado, Clean Camp and Rupestrian Cerrado (Oliveira *et al.*, 2007; Matos and Felfili, 2010). We employed a Geographic Information System to obtain information metrics[1].

Forest patrolling plays a pivotal role in safeguarding and overseeing these vital ecosystems, guaranteeing their well-being and conservation for generations to come. The deployment of robots in forest patrolling holds great significance, as it not only improves the effectiveness and safety of monitoring efforts but also plays an important role in conserving the rich biodiversity these ecosystems support, as previously noted by (Ferreira *et al.*, 2022a; Lima and Lima, 2014). In this context, we have swarm robotics that deals directly with multiple robots capable of performing a task in parallel, spending less time using controllers that guarantee this multi-agent approach.

Cellular automata (CA) and bioinspired computing offer intriguing opportunities for controlling robotics (Souza and Lima, 2019; Zeng *et al.*, 2022), with their applications extending to various domains, including autonomous navigation, swarm robotics, quantum computing and adaptive control systems (Gharaibeh *et al.*, 2020; Mordvintsev *et al.*, 2020). In this situation, cellular automata, a discrete compu-

---
[1]TerraBrasilis portal is a web platform developed by INPE for access, consultation, analysis and dissemination of geographic data `http://terrabrasilis.dpi.inpe.br/`.

tational model inspired by the behavior of biological systems, provide a framework for simulating and understanding complex, distributed processes (Monteiro *et al.*, 2020). The notion of local interactions and rule-based behaviors in cellular automata can be harnessed to govern robotic collectives and networks (Lopes and Lima, 2021). This is especially relevant in swarm robotics, where numerous simple robots work together, mirroring natural phenomena such as bird flocking or fish schooling.

Bio-inspired computing, on the other hand, draws inspiration from biological processes and organisms to devise novel algorithms and optimization techniques (Castello *et al.*, 2016). These methods often emulate the adaptive and intelligent behaviors observed in nature, such as genetic algorithms, neural networks and ant colony optimization (Dorigo *et al.*, 2006). When applied to robotics, bio-inspired algorithms can facilitate learning, adaptation, and problem-solving in dynamic and uncertain environments. For instance, ant colony optimization (ACO) can be used for perception and decision-making in robots, mimicking the ant colonies' structures and behaviors in search and exploration, using inverted pheromone approach techniques.

The integration of CA and bioinspired computing in robotics holds significant promise for creating more resilient, adaptive, efficient interactive robotic systems (Lima and Oliveira, 2017). Such approaches can enable robots to navigate complex and unpredictable terrains, collaborate in swarms for tasks like search and rescue, and optimize their operations through learning and evolution (Souza and Lima, 2019). Furthermore, these techniques contribute to the development of environmentally conscious robotics that can efficiently manage and conserve natural resources.

In this context, the objective of our work is to develop model control strategies for robotics using Cellular Automata and the pheromone-based optimization inspired by ant colony behavior to efficiently patrol and protect the vegetation in Sete Cidades National Park from the spread of wildfires. Such approaches can enable robots to navigate complex and unpredictable terrains, collaborate in swarms for tasks like search and rescue, and optimize their operations through learning and evolution. Furthermore, these techniques contribute to the development of environmentally conscious robotics that can efficiently manage and conserve natural resources.

2   Theoretical foundation

In this section, we will delve into the theoretical foundation that underpins the design and development of our innovative patrolling model for the Sete Cidades National Park within the Cerrado biome. This theoretical foundation consists of two fundamental pillars: cellular automaton and related works about swarm robotics control.

2.1   Cellular automata

Cellular automata are computational systems comprising sets of interacting cells, each represented by a state and following predetermined rules. Originally introduced as mathematical

models to simulate the intricacies of natural systems, including the one discussed in this article, CA operates on the fundamental concept of state transformations among neighboring cells (Alexan *et al.*, 2022). The system's evolution is contingent on transition rules, which can be either deterministic or probabilistic (Horibe *et al.*, 2021).

Cellular automaton can be depicted as either a vector or a matrix. They are categorized based on the number of dimensions in which their cells are organized. They can be one-dimensional, with cells arranged linearly, two-dimensional with cells forming a grid, or three-dimensional when the cells form a cube. CA consists of a set of cells (x_{ij}) within a lattice (L) of dimension (d), which can be updated over a specified time interval ($t \in T$). An example of a two-dimensional cellular automaton is Conway's Game of Life (GL), created by mathematician John Conway in 1970, as illustrated in Figure 1. The game is played on a grid of square cells, where each cell can be in one of two states: (1) alive, colorful, or (0) dead, in white. The rules of Conway's Game of Life are as follows: (i) any living cell with fewer than two living neighbors dies of loneliness; (ii) any live cell with two or three live neighbors continues to live in the next generation; (iii) any live cell with more than three live neighbors dies from overpopulation; (iv) any dead cell with exactly three live neighbors becomes a live cell. These rules are applied to each grid cell simultaneously to produce the next generation of cells. The game starts with an initial pattern of cells and then evolves from that pattern according to the game rules. The GL is an example of a complex dynamic system, with unpredictable emergent behavior based on simple rules.

Cellular automata are widely used in several areas of science to develop the spatial modeling of complex systems that have a large number of local interactions and that can exhibit unpredictable behavior, among them, we can mention forest modeling (Lima and Lima, 2014; Brasiel and Lima, 2023), modeling of diseases (Monteiro *et al.*, 2020), and even robotics control (Lopes and Lima, 2022), which is the focus of our work. Different works have already been proposed with the objective of create swarm robotics control through CA and using bio-inspired strategies, among them, we can mention the work of (Lopes and Lima, 2022) in which CA was used in a 2D form. In this article, we will explore their use in creating controllers, a complex process influenced by several variables, including the number of robots, vegetation type, pheromone and queues. CA can simulate these factors on a smaller scale, enabling more precise modeling of the controller's response to variations in the environment. This level of detail can contribute to the development of sophisticated control strategies and enhance the performance of various robotic systems.

2.2   Related works

In this subsection, we will provide an overview of robot navigation models based on two-dimensional cellular automata and their evolution. Additionally, we will offer a concise summary of the key characteristics of each model.

The initial model developed for swarm robotics in the context of surveillance tasks was the Inverted Ant Cellular Automata model, referred to as IACA, introduced by Lima *et al.*
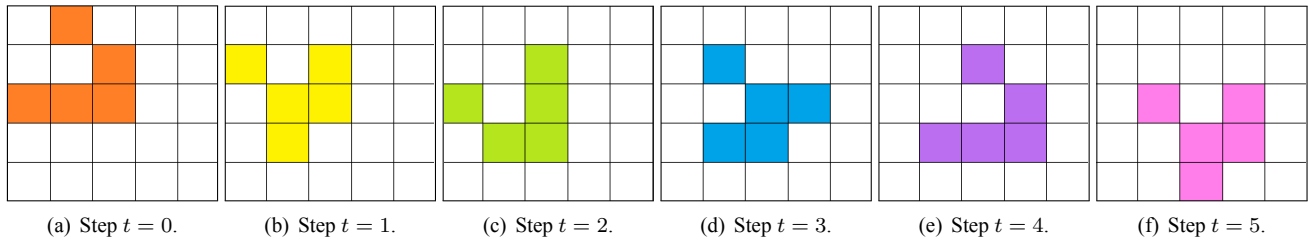
(a) Step $t = 0$.   (b) Step $t = 1$.   (c) Step $t = 2$.   (d) Step $t = 3$.   (e) Step $t = 4$.   (f) Step $t = 5$.

Figure 1. Time evolution by ($t = 6$) steps of the Game of Life, a two-dimensional cellular automaton created by John Conway in 1970.

(2016). The study incorporated four parameters, with an empirical alteration of the decay effect for comparison with the generic model introduced by Calvo *et al.* (2014), which was a navigation model for surveillance robots not utilizing cellular automata. In 2017, Tinoco *et al.* (2017) enhanced the earlier IACA model by introducing additional parameters to refine real-world experiments. This enhanced model was named Inverted Ant Cellular Automata with Discrete Pheromone Diffusion and Inertial Motion (IACA-DI). In this context, the Genetic Inverted Ant Cellular Automata (GIACA) model was implemented, further enhancing the IACA using a non-random Genetic Algorithm (GA), this GA was guided by biological and evolutionary strategies.

A meta-optimization approach based on genetic algorithms (GA) was investigated by Lopes and Lima (2021). In their subsequent work Lopes and Lima (2022), the model was referred to as Evolutionary with Genetic Algorithm for Inverted Ant Cellular Automata Discrete Inertia. This model was capable of refining parameters such as pheromone levels, evaporation rates, and the number of robots, among others, from precursor models (Lima *et al.*, 2016; Tinoco *et al.*, 2017). This GA implementation featured a distinct fitness function and a unique selection approach, generating a single offspring per crossover in each generation.

The adoption of Tabu search, inspired by the CAAM (Cellular Automata Ant Memory) robotic foraging task introduced by Lima and Oliveira (2017), led to the creation of TIACA (Tabu Inverted Ant Cellular Automata). TIACA incorporated a Tabu memory to assist in avoiding redundant paths for a single robot Souza and Lima (2019). There are other models that utilize the CA technique to address various problems in robotics. For instance, Ioannidis *et al.* (2011) focuses on solving the path-planning problem, while Lima and Oliveira (2017) addresses the issue of foraging task using swarm robotics. This model integrates local and global memory elements inspired by Tabu Search and genetic algorithms, leveraging evolutionary computation for optimization.

3   Proposal

In this section, we will introduce three models related to autonomous robot exploration of the environment. We will begin with a fundamental model that primarily employs cellular automata rules while considering vegetation probabilities. Next, we will delve into a model that incorporates the inverted pheromone concept from ant colonies. Finally, we will explore a model that integrates Tabu Search and Ants' Optimization for robot navigation.

3.1   General model description

This section outlines the model introduced here, which governs the operations of a robot responsible for environmental surveillance. The model described in this research draws inspiration from the precursor model known as Inverted Ants Cellular Automata, or simply IACA (Lima *et al.*, 2016). The primary distinction between our model proposed in this study and its precursor lies in the exploration of a map featuring various vegetation types. This map represents the Sete Cidades National Park, with a specific emphasis on forest fire surveillance. Besides that, we added a memory mechanism is influenced by the Tabu search technique (Glover, 1989, 1990).

3.1.1   Environment description

The spread of forest fires is significantly impacted by the type of vegetation present. Vegetation prone to ignition, such as dry grasslands and wood-rich forests, escalates the risk of rapid fire propagation. It is imperative to account for vegetation types during the modeling process because they directly influence robot mobility. For example, in denser vegetation, the robot is less likely to navigate through this vegetation. In riparian forests (humid vegetation, close to rivers) the robot should not navigate, as it could damage its monitoring components. On the other hand, in open savannah, the robot has a better chance of navigating, as there are not many obstacles in these regions. In the event of a fire, robots must accurately identify and navigate through these specific vegetation types along their trajectories.

To simulate the environment, we utilized an image depicting the primary vegetation of Sete Cidades National Park, as illustrated in Figure 2. Given the image's quality, we needed to preprocess its pixels for simulation by employing Euclidean distance calculations to identify color patterns through pixel color clustering. Applying robotics to environmental surveillance can be effectively achieved through realistic computer simulations. A prevalent software for two-dimensional (2D) spatial simulations of the environment (L CA-lattice) is Webots, which offers a lattice featuring cells where robots, drones, objects, and textures can be seamlessly integrated, as depicted in Figure 2.

For the implementation of robotic environmental surveillance, particularly in the context of the Sete Cidades National Park, a classification scheme with six distinct classes was established. Image segmentation is the process of dividing an image into regions based on specific criteria to identify objects, edges, colors, textures, or other visual features. Widely used in computer vision, image processing, and analysis, techniques and algorithms, relying on grayscale, tex-
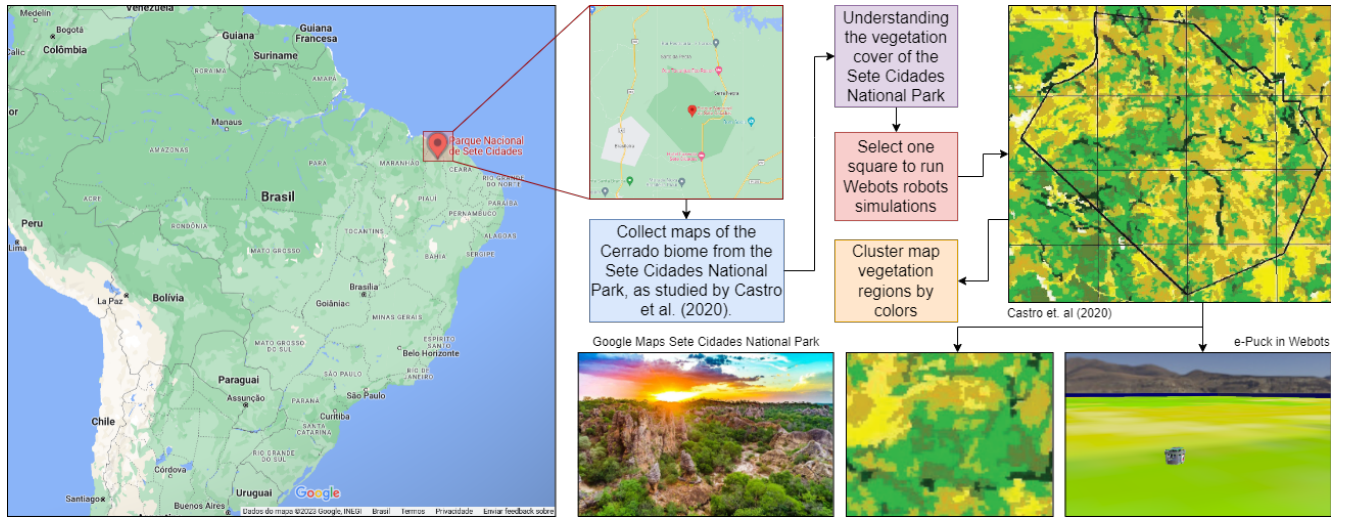
Figure 2. General modeling for the pre-processing and clustering stage of the Sete Cidades National Park environment for the e-Puck robot simulations in Webots.

tures or colors, divide the image into regions containing objects or features of interest, facilitating subsequent analysis. In our paper, class signifies a specific vegetation type, assigned based on the Euclidean distance calculated from the Red, Green and Blue (RGB) value of each pixel (Rodrigues *et al.*, 2022).

This method represents a clustering challenge, wherein data points are categorized into groups based on their similarity or proximity within a multi-dimensional space. In this context, it is a pixel clustering approach, aligning with the color schemes depicted in Figure 2. In this case, it helps identify and differentiate various types of vegetation, allowing for precise monitoring and management within the park. Six types of vegetation were used, including Riparian Forest, Evergreen Forest, Dense Cerrado, Typical Cerrado, Clean Camp and Rupestrian Cerrado (Alvarado *et al.*, 2019). After defining the class type, that is, the vegetation present in that pixel of the image, the pixel values were passed to a matrix. This matrix serves as a structured data representation where each cell corresponds to a pixel in the image and holds information about the vegetation class assigned to that pixel.

3.1.2 Computational structures description

Our model employs three 2-dimensional grids/computational matrices (CA-lattices) that mirror the dimensions and obstacles of the surveillance task environment. To begin, (a) an initial pheromone grid is created with all values initially set to zero. This grid is where the robot deposits, stores, and experiences pheromone evaporation along its path. Following this, (b) a physical CA-lattice represents the environmental Sete Cidades National Park, while (c) the last grid tracks the robot's current position. Additionally, two vectors are required to store the tabu positions queue for each robot present in the simulation.

It's essential to note that our proposed model exhibits both individual and global behaviors. The individual behavior pertains to the process of selecting the next robot movement, while the global behavior encompasses the robot's interaction with the grid and its surroundings. Both of these behaviors will be detailed in the subsequent subsections.

3.1.3 Robot individual behavior

The individual functionality of our model can be effectively depicted using a Finite State Machine (FSM), illustrated in Figure 3, using nine states and one gateway. A FSM serves as a mathematical model employed for depicting logical sequences or computer algorithms.

Initially, the robot is placed in a random location within the surveillance environment. Subsequently, it initiates a sequence of actions that persist from the initial choice of movement at time ($t = 0$) until the final time (T). This sequence commences by recording the current position into a circular queue (Q) implemented following the Tabu Search approach (Glover, 1989, 1990), which utilizes a first-in, first-out (FIFO) data structure, similar to what was employed in (Lima and Oliveira, 2017). In our model, this queue (Q) effectively prevents the robot from revisiting recently explored positions by maintaining a finite memory of such locations.

Subsequently, the robot assesses the neighboring cells, as defined by CA Moore's neighborhood (η^m). Moore's neighborhood signifies the number of cells in the CA neighborhood, represented as $\eta^m = (2r + 1)^2 - 1$, where its value is contingent on the radius (r). For instance, when CA-radius $r = 1$, the η^m value amounts to 8 neighboring cells. Within these neighboring cells, the robot deposits pheromones, a process governed by the pheromone deposition rate (δ) for the cells along the robot's cardinal lines and the dispersion rate (σ) for diagonal cells. The extent of pheromone deposited in each cell directly influences the probability ($P(x_{ij})$) of that cell being selected as the robot's next move. It's essential to ensure that the summation of the values being added to a cell at each time (see Equation 1) remains below a predefined maximum pheromone threshold ($\tau = 5 \times 10^3$).

$$\rho_{max}^t = \sum_{n=1}^{\eta^m} \rho(x_{ij})^t \qquad (1)$$

However, if any of the neighboring cells are recognized as obstacles, pheromone deposition is omitted in those cells. The current robot position is assigned a pheromone value of $\rho_{max} = \{1 \times 10^3, 2.5 \times 10^3, 4 \times 10^3\}$, indicating that this cell
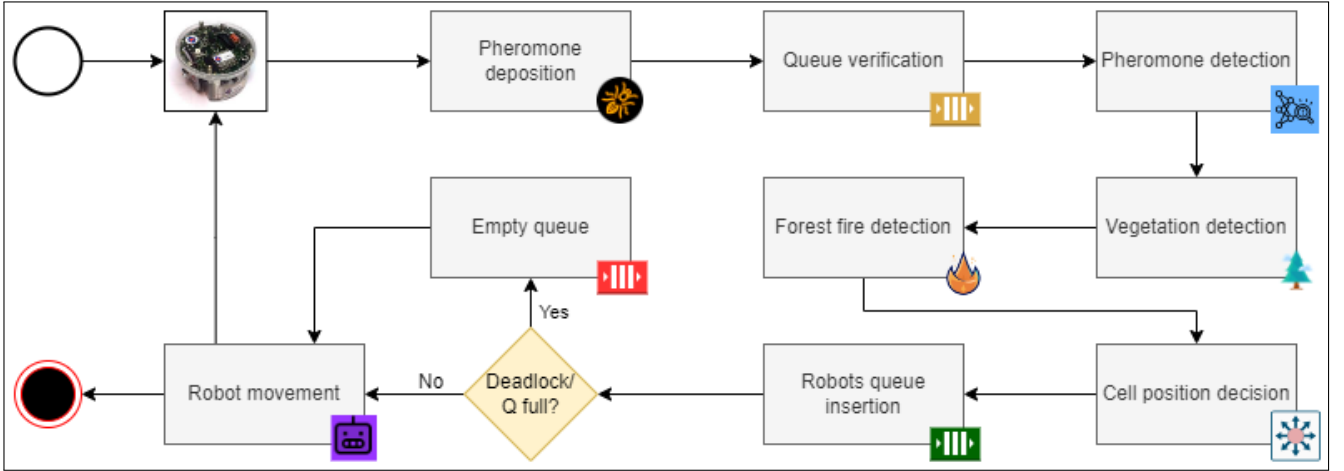
Figure 3. Robot individual behavior represented by a finite state machine, using 9 states and one decision gateway for alternative queue Q scenarios, considering e-Puck architecture.

might have been visited. High pheromone values in a cell correspond to a lower probability of it being selected, and vice versa. The probability of each cell (x_{ij}) being chosen by the robot in the next step, considers the vegetation class ($C_k, k \leq 6$), can be determined using Equation 2.

$$P(x_{ij})^{t+1} = \frac{c_k(x_{ij})^t \times (\rho_{max}^t - \rho(x_{ij})^t)}{\sum_{n=1}^{\eta^m} c_k(x_{ij})^t \times (\rho_{max}^t - \rho(x_{ij})^t)} \quad (2)$$

The subsequent action taken by the robot involves assessing the positions stored in the queue Q in comparison with the cells defined by Moore's neighborhood. This procedure identifies cells that have been recently visited by the robot. The incorporation of Q in the system yields improved task performance, specifically in terms of the number of coverage cycles completed by the robot within the environment. Equation 2 exclusively represents the available cells for the robot in the next step, excluding wall and queue cells. This numerical value corresponds to the probability of the robot's next move. This process iterates continuously until the predefined execution time T is attained.

3.1.4 Swarm Global behavior

The robot's collective behavior is determined by two primary factors: its interaction with the environment (indirect communication) and the pheromone evaporation process within the grids. While the addition of pheromone is localized to the robot's immediate neighborhood, the evaporation process is an ongoing operation that affects all cells within the environment, except those marked as obstacles. This evaporation process occurs at the end of each time step and is governed by a constant value ($\beta = 1$). The evaporation process is mathematically represented by Equation 3.

$$\rho(x_{ij})^{t+1} = \rho(x_{ij})^t - \beta \quad (3)$$

Figure 4 provides an illustrative environment that will be used to elucidate the comprehensive behavior of the robot. Figure 4(a) displays an environment being explored by a robot, showcasing the path taken by the robot, which is stored in queue Q, and the pheromone trail left behind by the robot's journey, similar to the behavior of ants. Remember that the

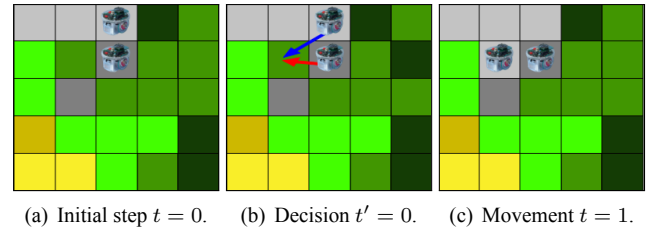(a) Initial step $t = 0$.   (b) Decision $t' = 0$.   (c) Movement $t = 1$.

Figure 4. Illustration of Robot Behavior, showing initial step at time $t = 0$, showing the robot's starting position, decision point at time $t' = 0$, where the robot selects its next move, movement step at time $t = 1$, depicting the robot's new position and possible movement choices.

concentration of pheromone is higher in the immediate vicinity of the robot's current position. This happens due to continuous pheromone evaporation in the environment, along with pheromone addition to adjacent cells when they directly contact the robot.

In the general case, the robot moves to the cell with the lowest value (least pheromone $\rho(x_{ij})$ and sparsest vegetation class c_k). However, at times, a robot may encounter two or more cells with equal probabilities, and in such cases, one of them is randomly selected. Another scenario involves conflicts where two or more robots (R_k) aim to move to the same cell. In this example, we have the e-Puck robot with a (R_1) blue arrow and the other (R_2) with a red arrow wanting to go to the same cell, as illustrated in the Figure 4(b). Finally, Figure 4(c) depicts the decision-making process during conflicts involving multiple robots. In these instances, only one robot (in this case, the blue one) is chosen to move, while the others remain stationary, maintaining their positions.

By examining the neighborhood cells included in queue Q, it's possible to determine if the robot has visited all available free positions. Thus, when facing an impasse, the controller resets queue Q to eliminate duplicate positions, preventing obstacles to the robot's movement (Lima and Oliveira, 2017). Once queue Q is cleared, it resumes storing positions from the reset point. In this study, we classify 3 robots as a swarm due to their collective emergent behavior, which enhances task efficiency over individual robots. This collective behavior enables the swarm to adapt, distribute tasks, and collaborate in real-time, thereby facilitating efficient environment patrolling.

3.2   Forest cellular automata random model

The initial model, known as the Forest Random Cellular Automata (FRCA) model, was developed to assess the robot's exploration behavior within the environment, particularly focusing on randomness. In this model, a robot denoted as R_k makes probabilistic movements based on the vegetation's probability values within its current cell x_{ij}. Different vegetation types were categorized into classes (C_i, where $i \leq 6$), namely: (c_1) Riparian Forest, (c_2) Evergreen Forest, (c_3) Dense Cerrado, (c_4) Typical Cerrado, (c_5) Clean Camp, and (c_6) Rupestrian Cerrado. Each vegetation type is associated with a specific probability $P(x_{ij})$, which determines the likelihood that robot R_k visits a two-dimensional CA lattice cell (x_{ij}) within lattice L. These probabilities are defined as $P(x_{ij}) = C_k(x_{ij})$. In this work we have different vegetation classes with different probabilities for robot movement $C_k(x_{ij}) = \{0.0, 0.7, 0.8, 0.9, 0.95, 1.0\}, k = 6$ for the respective vegetation types, according to Equation 4.

$$P(x_{ij})^{t+1} = c_k(x_{ij})^t \qquad (4)$$

For instance, in the case of Riparian Forest, the decision was made to exclude robot visits due to its dense vegetation and the low likelihood of fire spreading. This FCAR model's purpose is to evaluate how randomness in the robot's movement influences its interaction with different vegetation types and the potential impact on fire spread.

3.3   Forest inverted ant cellular automata model

However, confirming the need to improve the effectiveness of the surveillance mission and fire detection, it was decided to incorporate the Forest Inverted Ant Cellular Automata (FIACA) model, (Lima and Oliveira, 2017; Souza and Lima, 2019; Lopes and Lima, 2022). In both vegetation models they are represented within cells of a matrix 200×200 being saved in these cells in the vegetation class. It also has another matrix of the same dimension that contains the current positions of the robots. However, for the model based on the ant model, it was necessary to create another matrix to store the pheromone.

When the robot walks through a cell during its surveillance mission, it records that cell as visited and assigns an inverted pheromone value to that location in the matrix. To decide the next value, after some efficiency tests of the robot $R_k \in N$ (where N is the number of robots), it was decided that the maximum pheromone value would be 5×10^3 . In the first iteration, all vegetation receives the pheromone equal to 0, except in vegetation where the robot is prohibited from monitoring, which is assigned the value 5×10^3. Furthermore, in the main cell of the pheromone matrix the value $\{1 \times 10^3, 2.5 \times 10^3, 4 \times 10^3\}$ is added and in the surrounding cells the value 10^3 is added, so that it does not exceed the maximum pheromone value.

When planning its next move, the robot considers the inverted pheromone levels in neighboring cells $R_k \in \eta^m$. Cells with lower inverted pheromone values are considered more attractive, as they indicate that these areas have not yet

been sufficiently inspected. The movement calculation is carried out probabilistically according to the type of vegetation of the surrounding cells and the pheromone value of these cells. For each cell, a visit probability is assigned to the robot $R_k \in x_{ij}$, $P(x_{ij})$ using the Equation 3. After this, a cell is drawn based on the probability of the values and then the robot moves. Inverted pheromone levels in cells are dynamically updated with each iteration. As the robot continues its movement, the inverted pheromone values in the cells are decreased by $\beta = 1.0$ until reaching zero again if the robot does not pass that cell again during t iterations.

3.4   Forest tabu inverted ant cellular automata model

The implementation of the final Forest tabu inverted ant cellular automata model (FTIACA) involved the incorporation of "Tabu Search" into the ant inverted pheromone model as an essential element to optimize the robot's exploration path. One of the main features of Tabu Search in this context is the use of a two-dimensional queue Q to store the last positions visited by the robot. This queue acts as a short-term memory that records the coordinates (i, j) of the CA-grid cells x_{ij} where the robot recently passed, preventing the robot from returning to areas already inspected, saving time and resources.

The operation of the two-dimensional queue is relatively simple. When the robot moves to a new cell, the coordinates (i, j) of that cell are added to the corresponding queue with the value 1.0. However, the queue has a predefined maximum size. When it reaches its maximum $|Q|$ capacity (60 positions), the first element (the oldest cell) is removed, and the new coordinates are inserted at the end of the queue. In implementing the final model, a multiple robot system was also incorporated to further optimize the surveillance mission.

4   Methodology

In our paper, we employ a methodology rooted in the concept of CA and bioinspired computing to develop a novel approach for the robotics surveillance and patrolling of the Sete Cidades National Park within the Cerrado biome, that is possible to visualize in Figure 2. We developed our controller using the standard C language, specifically designed for the e-Puck robotic architecture. This controller is intended for use in the Webots simulator, which supports standard C language for development. Our work is quantitative because it primarily relies on the collection and analysis of numerical data to draw inferences, make conclusions, and support the findings presented in the study. We collected data from (Alvarado *et al.*, 2019), and we tested different parameters including the number of robots, pheromone levels, robot movements, and other quantitative metrics relevant to the surveillance task. We build upon the foundation of CA models, which are computational systems that consist of a CA-lattice of $|L| = 200 \times 200$ cells. Each cell evolves over time ($T = 10^4$ iterations) based on predefined rules and interactions with robots' neighboring cells. In our research, we adapt CA models to simulate the behavior and movement of robotic agents within the park,

and we used 10^2 simulations to have confidence in experiments. This modeling framework enables us to represent the environment as a grid, with each cell corresponding to a specific location within the park environment.

To make our CA model realistic and context-specific, we integrate environmental data related to the Sete Cidades National Park. This includes information about the park's geographical features, vegetation types ($C = 6$ vegetation classes), and fire risk factors. The incorporation of real-world data enhances the accuracy of our simulations and ensures that our approach is tailored to the park's unique characteristics. Our methodology also incorporates principles of swarm robotics control. We design and implement control algorithms that govern the behavior of robotic agents (robots) within the CA model. These algorithms dictate how robots move, make decisions, and respond to their environment. The swarm robotics approach allows multiple robots to work collaboratively and autonomously, emulating the behavior of natural swarms to enhance patrolling efficiency.

Specifically in our context, we do not employ more than three robots ($|R| = 3$) to accomplish the surveillance task. This constraint arises from the fact that the number of robots is intentionally kept smaller than the number of quadrants into which we virtually divide the Cartesian plane for monitoring the Sete Cidades National Park. The decision to maintain this balance is primarily influenced by the park's geographical layout and the intended division for efficient monitoring.

The virtual division (Cartesian plan) of the surveillance area into quadrants serves as an organizational strategy, ensuring that each robot is responsible for patrolling a specific region. When the number of robots equals or exceeds the number of quadrants, it can lead to an overlap of surveillance areas and inefficient resource allocation. In addition to consuming more hardware resources (e-Puck), which makes the approach not viable in terms of costs. This redundancy may result in robots revisiting areas that have already been patrolled or spending excessive time in the same locations, thus diminishing the overall efficiency of the surveillance mission.

By limiting the number of robots $|R|$ to less than the number of four-quadrants, we maintain a clear distribution of responsibilities and prevent redundancy in coverage (idle robots). Each robot is assigned initially in a unique area (virtual quadrant) to monitor, minimizing the chances of missing areas that require attention and optimizing the utilization of available resources. This approach is tailored to our specific surveillance task in the Sete Cidades National Park, enhancing the overall effectiveness of the robotic patrolling operation in Cerrado biome.

Building upon the success of bioinspired computing, we incorporate optimization techniques inspired by biological systems. One notable element is the use of ant colony optimization, which draws inspiration from the foraging behavior of ants. We implement ant-inspired pheromone trails to guide the robots in their patrolling tasks, helping them identify areas of interest and potential fire risks. Throughout our methodology, we emphasize rigorous performance evaluation. We quantify and analyze the effectiveness of our approach in patrolling the Sete Cidades National Park.

This evaluation includes measures such as coverage efficiency using Matlab program, more specifically coverage Steps and Pheromone rates using heatmaps with function `contourf(L)`, where each CA-grid $L(x_{ij})$ cell represents the mean of 10^2 simulations according to Equation 5.

$$L(x_{ij}) = \frac{\sum_{n=1}^{10^2} \sum_{k=1}^{T} x_{ij}}{10^2} \qquad (5)$$

Our methodology includes the use of statistical techniques and tools such as box plots, means, medians, quartiles, and other numerical representations to analyze the data, using the BoxPlotR[2]. The results of our analysis provide valuable insights into the practicality and efficiency of our proposed approach. By combining cellular automata modeling, environmental data integration, swarm robotics control, bioinspired optimization, and rigorous performance evaluation, our methodology offers a comprehensive framework for improving the surveillance and patrolling of the Sete Cidades National Park, ultimately contributing to the protection of this unique natural environment.

5   Results

In this section, we will delve into three essential aspects of our research: model variation, the impact of varying the number of robots, and the influence of the maximum amount of pheromone per cell on our experimental results.
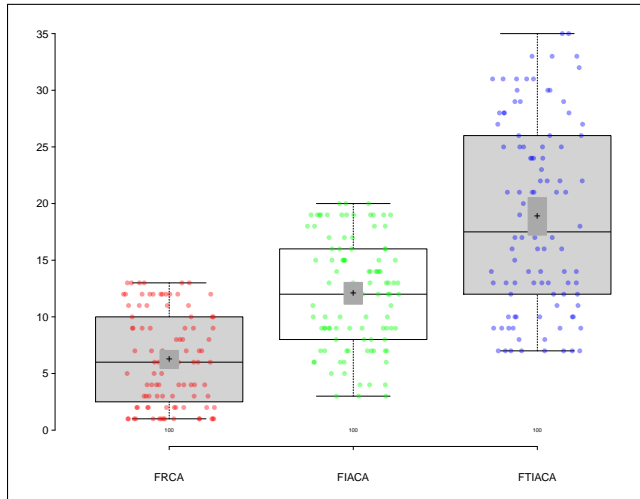
5.1   Model variation

The box plot statistics provided for the three models, FRCA, FIACA, and FTIACA, offer valuable insights into the distribution and central tendency of the data. Figure 5 with these statistics help us understand the performance variation among these models for the simulated task of patrolling Sete Cidades National Park in a Cerrado biome, considering $R = 3$ robots, maximum amount of pheromone $\tau = 2500$ (except for random model), evaporation tax $\beta = 1$, and $|Q| = 80$ (only for FTIACA). At each time step, 1500 units of pheromone are deposited into the central cell $\rho(x_{ij})^{max}$, while in its neighboring cells, marked as $\rho(x_{ab})$, where $a, b \in \eta^m$ and considering a CA-radius of $r = 1$, 750 units of pheromone are deposited. The upper whisker, which represents the maximum value within 1.5 times the interquartile range (IQR) above the third quartile, is highest for FTIACA at 35.00, indicating some relatively higher outlier data points, as is possible to observe on Table 1. In contrast, FRCA and FIACA have upper whisker values of 13.00 and 20.00, respectively. This implies that the FTIACA model exhibits greater variability in its performance with some notably high values.

The median, a measure of central tendency, offers insights into the model's typical or central performance. In this case, FTIACA has the highest median of 17.50, indicating that it tends to perform relatively well on the task. FIACA follows with a median of 12.00, while FRCA has the lowest median

---

[2]BoxPlotR: a web-tool for generation of box plots `http://shiny.chemgrid.org/boxplotr/`.

Table 1. Statistics comparison of surveillance performance varying different models, robot numbers and maximum pheromone levels.

Statistics	FRCA Model	FIACA Model	FTIACA Model	1 Robot	2 Robots	3 Robots	Pheromone 1000	Pheromone 2500	Pheromone 4000
Upper whisker	13.00	20.00	35.00	5.00	13.00	35.00	40.00	35.00	34.00
3rd quartile	10.00	16.00	26.00	2.00	7.00	26.00	29.00	26.00	24.50
Median	6.00	12.00	17.50	1.00	5.00	17.50	21.00	17.50	15.50
1st quartile	2.50	8.00	12.00	0.00	2.00	12.00	15.00	12.00	10.50
Lower whisker	1.00	3.00	7.00	0.00	0.00	7.00	7.00	7.00	7.00
Mean	6.24	12.08	18.87	1.28	5.20	18.87	21.77	18.87	17.49
Nr. of data points	100.00	100.00	100.00	100.00	100.00	100.00	100.00	100.00	100.00

Figure 5. Boxplots for three models variations.

of 6.00, suggesting that FTIACA shows the best central performance, FIACA follows, and FRCA exhibits the lowest central performance among the three models. The mean values provide further insight, represented by $(+)$ inside the box plot, confirming these trends in central performance. Herein we used the 95.0% confidence interval, represented by (■) in box plot, which is an estimate of an interval used in statistics, which contains a population parameter. This result is found through a sampling model calculated from the collected data. FTIACA's mean of 18.87 is the highest, followed by FIACA with 12.08, and FRCA with the lowest mean of 6.24. Overall, these statistics reveal that FTIACA tends to perform well on average, but its performance exhibits more variability with some high outliers, while FRCA generally has lower and less variable performance, as indicated by its lower median and mean.

To evaluate the pheromone coverage in the environment for the FIACA and FTIACA models, we created a heatmap in Matlab according to Figure 6, facilitating a qualitative analysis. The temperature of each cell was calculated by the arithmetic mean of each of the 10^2 simulations carried out over $T = 10^4$ iterations. The heatmap reveals a distinct distribution of accumulated pheromone between the two models. Notably, the FTIACA model exhibits a higher accumulation of pheromone (see Figure 6(a)) when compared to FIACA (see Figure 6(b)), indicating a more effective and efficient coverage strategy. The areas in black throughout the heatmap result from areas of Riparian Forest, a dense and humid portion with a low probability of burning, and which are considered obstacles for robots (see Figure 2). However, upon closer inspection, we notice that the FIACA model exhibits
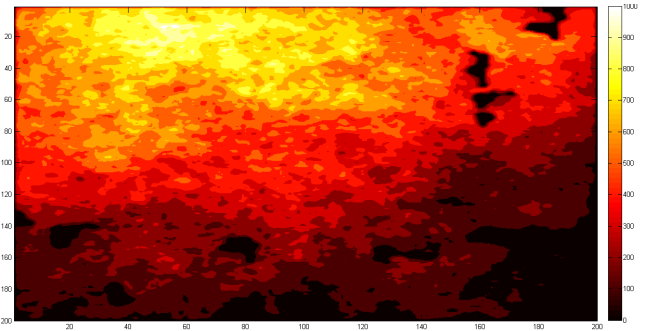
(a) Pheromone heatmap for FIACA model.
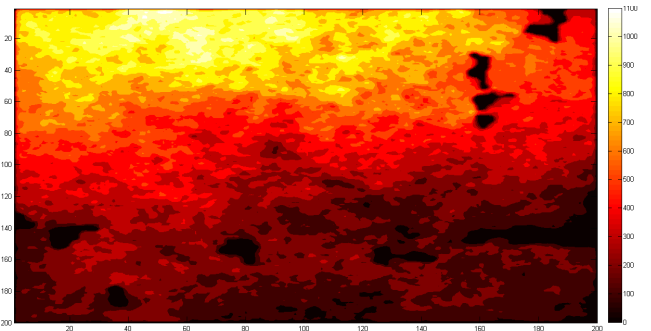
(b) Pheromone heatmap for FTIACA model.

Figure 6. Mean of Pheromone Heatmaps for FIACA and FTIACA Models.

a higher prevalence of non-recently visited points, evident by the darker regions on the heatmap. This suggests that in FIACA, there was a challenge in achieving an optimal distribution of robots to uniformly cover the environment.

We then generated a heatmap illustrating the average number of steps taken per cell by each robot over 10^2 simulations with a duration of $T = 10^4$. The analysis of these heatmaps reveals important insights into the characteristics of the three models used in our research, according to Figure 7. The FRCA model, characterized by its randomness, relies primarily on differing probabilities associated with navigating through various types of vegetation within the Sete Cidades National Park. This probabilistic approach reflects a less structured strategy, see Figure 7(a). The FIACA model introduces a level of indirect communication among robots by considering the probabilities of robot movement through each vegetation type and utilizing the inverted pheromone left as a trail along their paths. This allows for a more coordinated and intelligent patrolling strategy, see Figure 7(b).

The FTIACA model, being the most advanced, considers movement probability in relation to vegetation, pheromone levels, and queue usage, leading to heightened vigilance, especially in fire-prone areas, see Figure 7(c). These per-
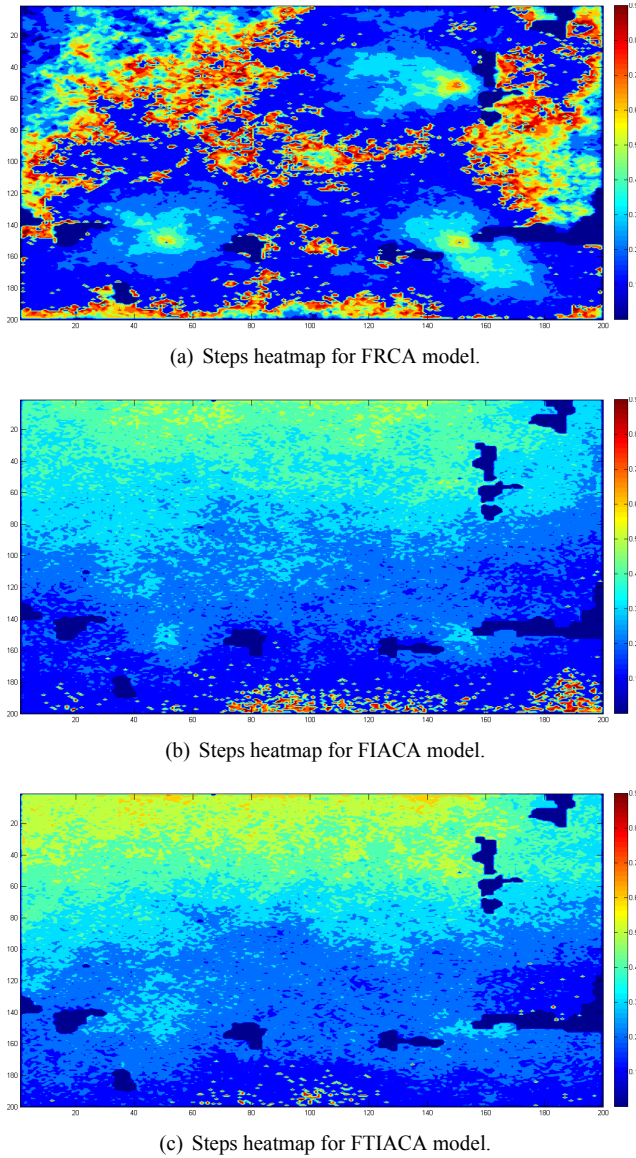
(a) Steps heatmap for FRCA model.

(b) Steps heatmap for FIACA model.

(c) Steps heatmap for FTIACA model.

Figure 7. Mean of Steps Heatmaps for FRCA, FIACA and FTIACA Models.

formance differences emphasize the value of sophisticated strategies in swarm robotics for patrolling and environmental surveillance, enhancing robot distribution for improved environmental protection.

5.2 Number of robots variation

For the experiments in this section, it is important to consider that in the central cell, the amount of pheromone is $\rho(x_{ij})^{max} = 1500$, while in its neighboring cells, the amount is $\rho(x_{ab}) = 750$ units, where $a, b \in \eta^m$, taking into account a CA-radius of $r = 1$ and $|Q| = 80$. The box plot statistics for the number of robots variation, with 1, 2, and 3 robots patrolling the Sete Cidades National Park in the Cerrado biome, offer significant insights into the impact of the number of robots on task performance, as is possible to observe in Figure 8. These statistics inform the impact of varying robot numbers on data tendencies and distributions, serving as a foundation for informed discussion.

The upper whisker demonstrates a consistent increase in maximum performance with rising robot numbers. With 1
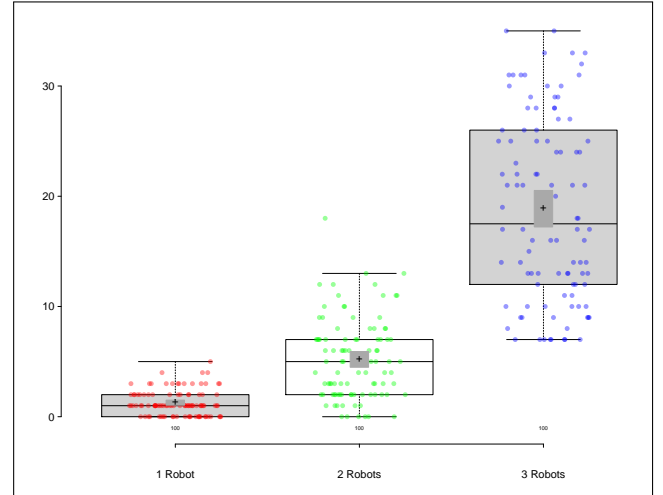
Figure 8. Boxplots for robots number variations.

robot, it's at 5.00, rising to 13.00 with 2 robots, and significantly increasing to 35.00 with 3 robots. This indicates that adding more robots enhances performance potential, especially in extreme cases. The median follows a similar trend, with values of 1.00 for 1 robot, 5.00 for 2 robots, and 17.50 for 3 robots, signifying improved patrolling performance on average with more robots. The mean performance, which is 1.28 with 1 robot, increases to 5.20 with 2 robots and further to 18.87 with 3 robots.

The Figure 9 presents pheromone heatmaps for different numbers of robots in the FTIACA model, providing valuable insights into the impact of robot quantity on pheromone coverage. As we evaluate the patterns depicted in these heatmaps, several significant trends and implications emerge. First, as we transition from one to two robots, the pheromone heatmap (Figures 9(a) and 9(b)) indicates that the presence of additional robots substantially increases pheromone accumulation in the environment. The collective effort of two robots improves pheromone distribution, especially near their positions. Higher pheromone concentration aids in better environmental surveillance for fire detection and prevention.
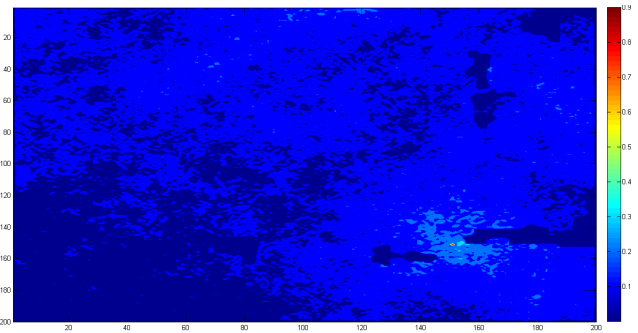
When we further scale up to three robots (Figure 9(c)), the trend of increased pheromone accumulation continues. The coverage becomes even more extensive, reaching deeper into the environment. These observations highlight that a higher number of robots offers substantial advantages for pheromone-based patrolling strategies. This results in a broader scope of surveillance across the entirety of Sete Cidades National Park, thereby enhancing the overall effectiveness and efficiency of the FTIACA model.

Figure 10 illustrates steps heatmaps in the FTIACA model with varying robot numbers. These heatmaps provide insights into how the number of robots affects movement distribution in the surveillance environment. The heatmap for one robot (Figure 10(a)) shows limited environmental coverage. The heatmap shows limited steps taken by a single robot to traverse the entire area, reflecting the challenge of a single robot effectively patrolling a large and complex environment. While there is coverage in various regions, there are significant gaps that could lead to a decreased ability to detect and prevent potential fires.
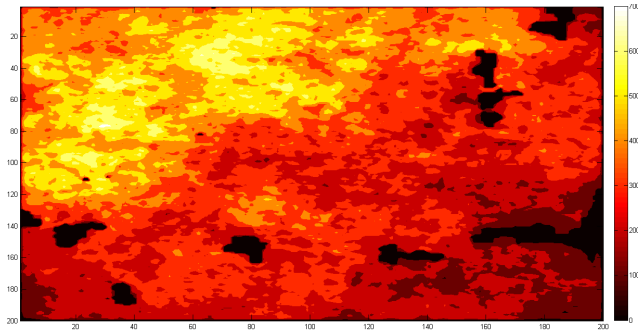
As we introduce a second robot (Figure 10(b)), the heatmap illustrates a substantial improvement in terms of
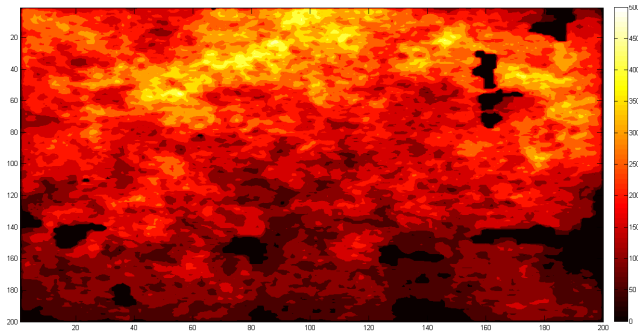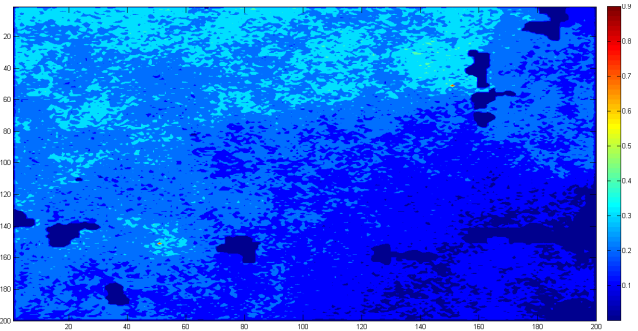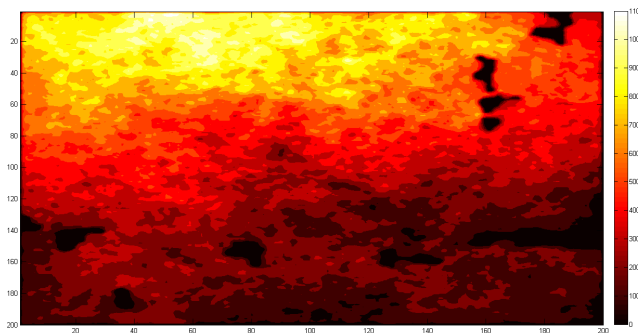
(a) Pheromone heatmap for 1 robot.
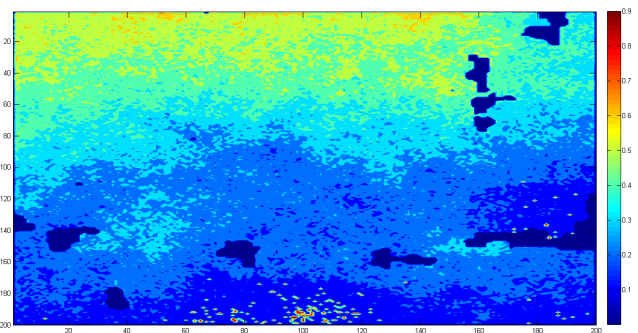

(b) Pheromone heatmap for 2 robots.

(c) Pheromone heatmap for 3 robots.

Figure 9. Mean of Pheromone Heatmaps for FTIACA varying robots number.

(a) Steps heatmap for 1 robot.

(b) Steps heatmap for 2 robots.

(c) Steps heatmap for 3 robots.

Figure 10. Mean of Steps Heatmaps for FTIACA varying robots number.

coverage. There is a significant reduction in untraversed areas, and the robots collectively patrol the environment more thoroughly. The movement patterns overlap, resulting in better surveillance, which contributes to the early detection of potential fire hazards. Expanding to three robots (Figure 10(c)), the heatmap demonstrates further improvements in coverage. Increased robot numbers lead to more efficient patrolling, reflected in higher median and mean values. While a wider upper whisker hints at potential exceptional performance in certain cases, it also introduces greater variability. Deploying additional robots improves patrolling in Sete Cidades National Park, lowering the risk of overlooking critical areas and boosting overall fire prevention efficiency. The FTIACA model showcases superior environmental coverage, as seen in the pheromone and step heatmaps.

5.3　Amount of pheromone variation

The Forest Tabu Inverted Ant Cellular Automata (FTIACA) model, which incorporates the concept of pheromone trails inspired by the behavior of ants, plays a critical role in the context of robotic surveillance within the Sete Cidades National Park. This model introduces the notion of a maximum virtual amount of pheromone that robotic agents can deposit and utilize during their patrolling tasks. The examination of box plot statistics for three different scenarios with varying maximum pheromone levels $\tau = 1000$ (where $\rho(x_{ij}) = 600, \rho(x_{ab}) = 300$), $\tau = 2500$ (where $\rho(x_{ij}) = 1500, \rho(x_{ab}) = 750$), and $\tau = 4000$ (where $\rho(x_{ij}) = 2500, \rho(x_{ab}) = 1500$) provides valuable insights into the performance and efficiency of the IACA model, considering $|Q| = 80$.

The box plot statistics clearly reveal how different maximum pheromone levels impact the performance of the FTIACA model in the surveillance of Sete Cidades National Park, as is shown in Figure 11. As the maximum pheromone level increases from 1000 to 2500 and 4000, several trends emerge. Notably, upper whisker, third quartile, and median values consistently decrease, suggesting a narrower data range and more controlled patrolling. The FTIACA model demonstrates adaptability and effectiveness in a dynamic environment, with a higher maximum pheromone level enhancing task efficiency. Constant lower whisker values at 7.00
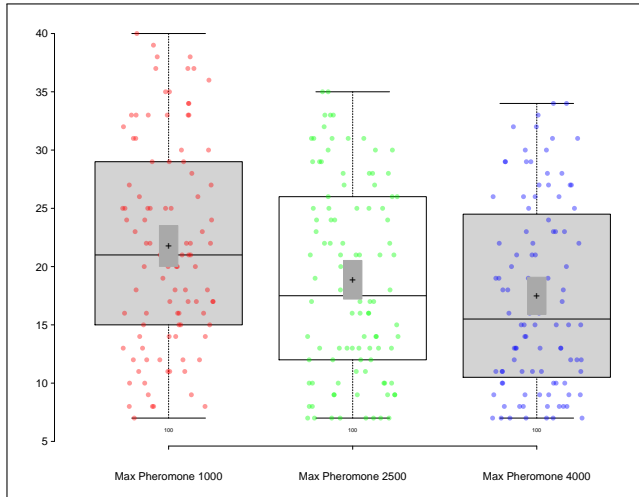
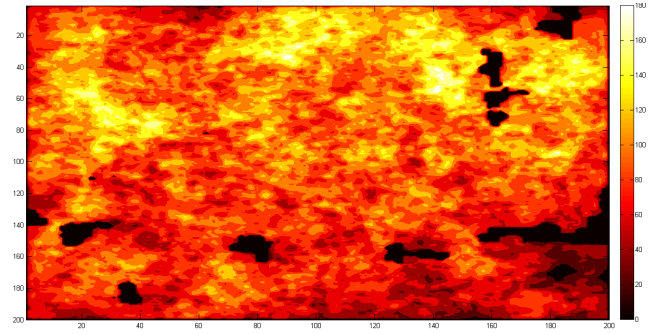**Figure 11.** Boxplots for maximum amount of pheromone variation.

reveal the minimum pheromone level required for a functional system. Mean values show a decreasing trend at higher pheromone levels but remain close to mid-range data values.

The Figure 12 reveals how variations in the maximum amount of pheromone per cell influence the distribution and accumulation of pheromone in the FTIACA model, shedding light on the model's performance under different pheromone conditions. Figure 13 shows the average number of steps based on the variation in the maximum amount of pheromone that can be deposited per cell. In the scenario with the lowest maximum pheromone per cell (1000 units), as shown in Figure 12(a), the heatmap displays notable pheromone accumulation, averaging 180 units per cell. Figure 13(a) illustrates the step count per cell, indicating effective environmental coverage, although some accumulation points are visible. Even with limited pheromone supply, robots efficiently deposit pheromone, contributing to substantial coverage. More robots in the area lead to denser pheromone deposition. In the scenario with a moderate maximum pheromone per cell (2500 units), depicted in Figure 12(b), the heatmap shows a significant increase in pheromone accumulation, averaging 1100 units per cell. Figure 13(b) displays step coverage, which is less efficient than the scenario with lower pheromone usage, demonstrating a less effective pheromone distribution, albeit with enhanced surveillance capabilities.

Additional pheromone availability does not improve patrolling effectiveness. In the scenario with the highest maximum pheromone per cell (4000 units), shown in Figure 12(c), the heatmap displays substantial pheromone accumulation, averaging 2000 units per cell. However, Figure 13(c) indicates suboptimal step coverage, with robot clusters on the bottom right side. This scenario results in the poorest pheromone coverage, indicating that increasing the maximum pheromone per cell did not enhance environmental coverage or task completion rates.
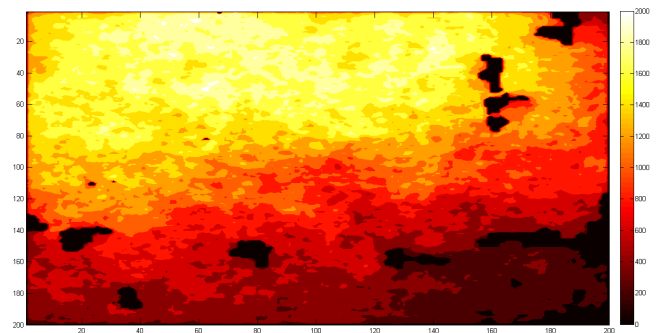
6   Discussion

The FTIACA model, incorporating the Queue and Tabu mechanism, optimizes robot distribution to enhance pheromone coverage and overall surveillance efficiency, thereby improving environmental protection. Furthermore,

(a) Pheromone heatmap at 1000 units per cell.
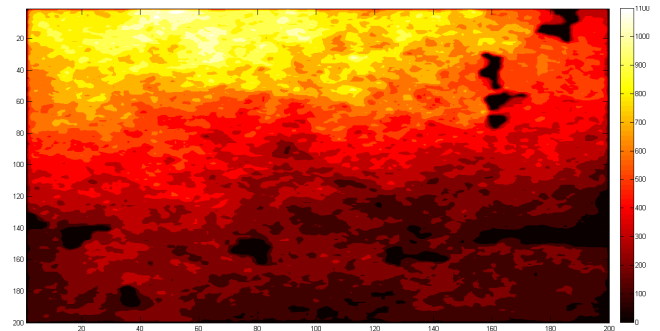
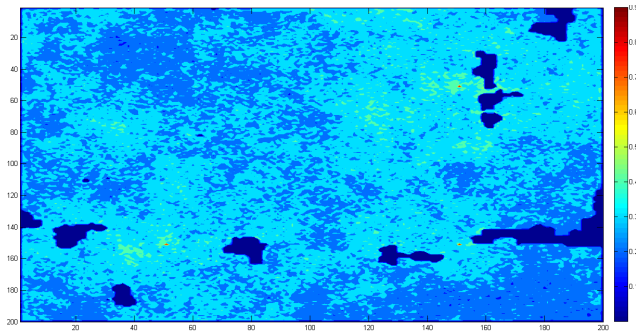(b) Pheromone heatmap at 2500 units per cell.
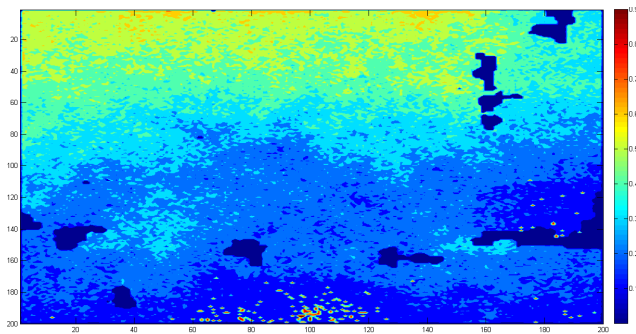

(c) Pheromone heatmap at 4000 units per cell.

Figure 12. Mean of Pheromone Heatmaps for FTIACA considering variations for maximum amount of pheromone per cell.

the pheromone heatmaps vividly demonstrate the direct link between robot quantity and pheromone coverage. Increased robots result in superior pheromone distribution, underscoring the necessity of optimizing robot numbers in the FTIACA model for enhanced environmental protection, echoing findings from previous studies Lima *et al*. (2016); Lopes and Lima (2022). Increasing robot numbers in FTIACA significantly enhances surveillance efficiency, reducing unpatrolled areas and improving fire detection and prevention in Sete Cidades National Park. These heatmaps also demonstrate the impact of maximum pheromone levels on FTIACA's performance. Unlike previous studies Souza and Lima (2019); Lima and Oliveira (2017); Lopes and Lima (2021), we integrate Sete Cidades National Park's vegetation classes, influencing swarm robotics movement. Higher pheromone availability enhances environmental coverage, underscoring the importance of optimizing pheromone resources for effective patrolling in real-world scenarios.
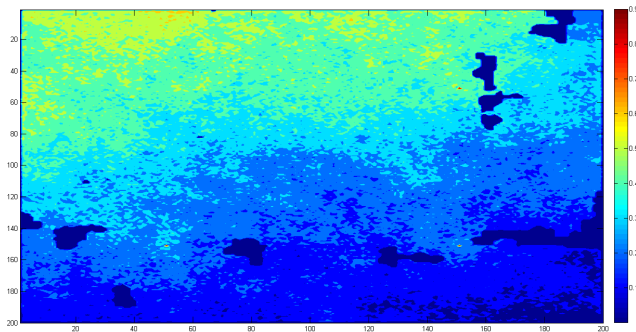
We chose Matlab and the e-Puck environment for their suitability to our research goals and available features.

(a) Steps heatmap for maximum amount of pheromone per cell equals to 1000.

(b) Steps heatmap for maximum amount of pheromone per cell equals to 2500.

(c) Steps heatmap for maximum amount of pheromone per cell equals to 4000.

Figure 13. Mean of Pheromone Heatmaps for FTIACA considering variations for maximum amount of pheromone per cell.

While we recognize the benefits of open-source alternatives, none fully met our requirements or offered comparable functionalities. An inherent limitation of our study is the cost of the e-Puck, along with its small and delicate nature, which may pose challenges considering the specified task.

7   Conclusions

The preservation of the Cerrado's ecosystem is vital for Brazil and swarm robotics patrols protect this biome by monitoring, detecting threats like wildfires, The preservation of the Cerrado's unique ecosystem is vital for Brazil. The results unequivocally showcase the Forest Tabu Inverted Ant Cellular Automata (FTIACA) as the top-performing model, achieving an impressive average of 21.77 complete patrol cycles, with a high 95% confidence level. This remarkable performance was realized through the orchestration of three robots, a Tabu queue set at $|Q| = 80$, and the utiliza-

tion of a maximum pheromone amount per cell set to $\rho = 1000$. These parameter configurations highlight the model's remarkable ability to optimize patrol cycles and resource utilization, particularly in the crucial context of fire prevention in Sete Cidades National Park. In summary, the fusion of cellular automata and bioinspired computing presents a promising path for advancing robotics and its diverse applications.

In future research, we aim to analyze Sete Cidades National Park further, utilizing drones to capture imagery of its upper regions. Additionally, we plan to use e-Pucks to acquire images for Virtual and Augmented Reality applications, as discussed by (Sanches *et al.*, 2019). Furthermore, the work may involve the optimization analysis of model hyperparameters using genetic algorithms.

Acknowledgements

References

Alencar, J., Cordeiro, W. P. F. d. S., Staples, G., and Buril, M. T. (2019). Convolvulaceae no parque nacional de sete cidades, estado do piauí, brasil. *Hoehnea*, 46:e992018. DOI: https://doi.org/10.1590/2236-8906-99/2018.

Alexan, W., ElBeltagy, M., and Aboshousha, A. (2022). Rgb image encryption through cellular automata, s-box and the lorenz system. *Symmetry*, 14(3):443. DOI: https://doi.org/10.3390/sym14030443.

Alvarado, S., Carvalho, I., Ferraz, T., and Silva, T. (2019). Effects of fire suppression policies on fire regimes in protected areas in the cerrado. *Biodiversidade Brasileira-BioBrasil*, (1). DOI: https://doi.org/10.37002/biodiversidadebrasileira.v9i1.1143.

Brasiel, H. C. and Lima, D. A. (2023). Exploring the influence of wind, vegetation and water sources on the spread of forest fires in the brazilian cerrado biome using cellular automata. In *Anais do XIV Workshop de Computação Aplicada à Gestão do Meio Ambiente e Recursos Naturais*, pages 61–70. SBC. DOI: https://doi.org/10.5753/wcama.2023.230476.

Calvo, R., de Oliveira, J. R., Figueiredo, M., and Romero, R. A. (2014). Parametric investigation of a distributed strategy for multiple agents systems applied to cooperative tasks. In *Proceedings of the 29th Annual ACM Symposium on Applied Computing*, pages 207–212. ACM. DOI: https://doi.org/10.1145/2554850.2554977.

Castello, E., Yamamoto, T., Dalla Libera, F., Liu, W., Winfield, A. F., Nakamura, Y., and Ishiguro, H. (2016). Adaptive foraging for simulated and real robotic swarms: the dynamical response threshold approach. *Swarm Intelligence*, pages 1–31. DOI: https://doi.org/10.1007/s11721-015-0117-7.

Dorigo, M., Birattari, M., and Stutzle, T. (2006). Ant colony optimization. *IEEE computational intelli-*

gence magazine, 1(4):28–39. DOI: https://doi.org/10.1109/MCI.2006.329691.

Ferreira, M. E. A., Lima, D. A., Martins, L. G., and Oliveira, G. M. (2022a). Refining a parameter setting evolutionary approach for fire spreading models based on cellular automata. In *2022 International Conference on Computational Science and Computational Intelligence (CSCI)*, pages 480–486. IEEE. DOI: https://doi.org/10.1109/CSCI58124.2022.00091.

Ferreira, M. E. A., Quinta, A. L., Lima, D. A., Martins, L. G., and Oliveira, G. (2022b). Automatic evolutionary adjustment of cellular automata model for forest fire propagation. In *International Conference on Cellular Automata for Research and Industry*, pages 235–245. Springer. DOI: https://doi.org/10.1007/978-3-031-14926-9_21.

Gaia, J. A. S., Souza, B. I. d., Lucena, R. F. P. d., Souza, R. S., and Gaia, C. L. B. (2022). Modelagem e distribuição potencial de espécies arbóreas relevantes para a dinâmica sociocultural e ecológica do parque nacional de sete cidades, piauí, brasil. *Sociedade & Natureza*, 32:784–798. DOI: https://doi.org/10.14393/SN-v32-2020-51103.

Gharaibeh, A., Shaamala, A., Obeidat, R., and Al-Kofahi, S. (2020). Improving land-use change modeling by integrating ann with cellular automata-markov chain model. *Heliyon*, 6(9). DOI: https://doi.org/10.1016/j.heliyon.2020.e05092.

Glover, F. (1989). Tabu search part i. *ORSA Journal on computing*, 1(3):190–206. DOI: https://doi.org/10.1287/ijoc.1.3.190.

Glover, F. (1990). Tabu search part ii. *ORSA Journal on computing*, 2(1):4–32. DOI: https://doi.org/10.1287/ijoc.2.1.4.

Horibe, K., Walker, K., and Risi, S. (2021). Regenerating soft robots through neural cellular automata. In *Genetic Programming: 24th European Conference, EuroGP 2021, Held as Part of EvoStar 2021, Virtual Event, April 7–9, 2021, Proceedings 24*, pages 36–50. Springer. DOI: https://doi.org/10.1007/978-3-030-72812-0_3.

Ioannidis, K., Sirakoulis, G. C., and Andreadis, I. (2011). A path planning method based on cellular automata for cooperative robots. *Applied Artificial Intelligence*, 25(8):721–745. DOI: https://doi.org/10.1080/08839514.2011.606767.

Lima, D. A. and Oliveira, G. M. (2017). A cellular automata ant memory model of foraging in a swarm of robots. *Applied Mathematical Modelling*, 47:551–572. DOI: https://doi.org/10.1016/j.apm.2017.03.021.

Lima, D. A., Tinoco, C. R., and Oliveira, G. M. B. (2016). A cellular automata model with repulsive pheromone for swarm robotics in surveillance. In *Cellular Automata - International Conference on Cellular Automata for Research and Industry, ACRI. Proceedings*, pages 312–322. DOI: https://doi.org/10.1007/978-3-319-44365-2_31.

Lima, H. A. and Lima, D. A. (2014). Autômatos celulares estocásticos bidimensionais aplicados a simulação de propagação de incêndios em florestas homogêneas. In *Anais do V Workshop de Computação Aplicada a Gestão do Meio Ambiente e Recursos Naturais*, pages 15–24. SBC. DOI: https://doi.org/10.13140/RG.2.1.4578.8564.

Lopes, H. J. and Lima, D. A. (2021). Evolutionary tabu inverted ant cellular automata with elitist inertia for swarm robotics as surrogate method in surveillance task using e-puck architecture. *Robotics and Autonomous Systems*, page 103840. DOI: https://doi.org/10.1016/j.robot.2021.103840.

Lopes, H. J. and Lima, D. A. (2022). Surveillance task optimized by evolutionary shared tabu inverted ant cellular automata model for swarm robotics navigation control. *Results in Control and Optimization*, 8:100141. DOI: https://doi.org/10.1016/j.rico.2022.100141.

Matos, M. d. Q. and Felfili, J. M. (2010). Florística, fitossociologia e diversidade da vegetação arbórea nas matas de galeria do parque nacional de sete cidades (pnsc), piauí, brasil. *Acta botânica brasílica*, 24:483–496. DOI: https://doi.org/10.1590/S0102-33062010000200019.

Monteiro, L., Fanti, V., and Tessaro, A. (2020). On the spread of sars-cov-2 under quarantine: A study based on probabilistic cellular automaton. *Ecological Complexity*, 44:100879. DOI: https://doi.org/10.1016/j.ecocom.2020.100879.

Mordvintsev, A., Randazzo, E., Niklasson, E., and Levin, M. (2020). Growing neural cellular automata. *Distill*, 5(2):e23. DOI: https://doi.org/10.23915/distill.00023.

Oliveira, M. E. A., Martins, F. R., Castro, A., and Santos, J. d. (2007). Classes de cobertura vegetal do parque nacional de sete cidades (transição campo-floresta) utilizando imagens tm/landsat, ne do brasil. *XIII Simpósio Brasileiro de Sensoriamento Remoto*, 13.

Rodrigues, L. G. S., Dias, D. R. C., de Paiva Guimarães, M., Brandão, A. F., Rocha, L. C., Iope, R. L., and Brega, J. R. F. (2022). Supervised classification of motor-rehabilitation body movements with rgb cameras and pose tracking data. *Journal on Interactive Systems*, 13(1):221–231. DOI: https://doi.org/10.5753/jis.2022.2409.

Sanches, S. R., Oizumi, M. A., Oliveira, C., Sementille, A. C., and Corrêa, C. G. (2019). The influence of the device on user performance in handheld augmented reality. *Journal on Interactive Systems*, 10(1). DOI: https://doi.org/10.5753/jis.2019.718.

Souza, N. L. B. and Lima, D. A. (2019). Tabu search for the surveillance task optimization of a robot controlled by two-dimensional stochastic cellular automata ants model. In *Latin American Robotics Symposium, Brazilian Symposium on Robotics and Workshop on Robotics in Education*, pages 299–304. IEEE. DOI: https://doi.org/10.1109/LARS-SBR-WRE48964.2019.00059.

Tinoco, C. R., Lima, D. A., and Oliveira, G. M. (2017). An improved model for swarm robotics in surveillance based on cellular automata and repulsive pheromone with discrete diffusion. *International Journal of Parallel, Emergent and Distributed Systems*, 34(1):53–77. DOI: https://doi.org/10.1080/17445760.2017.1334886.

Zeng, J., Qian, Y., Yin, F., Zhu, L., and Xu, D. (2022). A multi-value cellular automata model for multi-lane traffic flow under lagrange coordinate. *Computational and Mathematical Organization Theory*, pages 1–15. DOI: https://doi.org/10.1007/s10588-021-09345-w.